Chapter 3
Multi-objective Optimization Strategies

Abstract In this chapter, multi-objective optimization as a strategy for quality production of parts through fused deposition modelling is presented. Various techniques used in undertaking the multi-objective optimization process are described based on case studies from the literature and the authors' data. The general algorithms for multi-objective optimization of the FDM process are described. The most significant objectives of the various optimization cases are identified and described in relation to the quality of the fused deposition modelling of parts. The main objectives for optimizing fused deposition process are (i) to increase the rate of production, (ii) to reduce material wastage and utilize as minimum material as possible, (iii) save on the cost of power consumption during printing and (iv) achieve the highest quality of FDM parts.

Keywords 3D printing · Fused deposition modelling · Genetic algorithms · Grey relational degree · Multi-objective optimization · Pareto · Printing parameters

3.1 Introduction

Optimization generally involves determining the maximum or minimum value considering one or several objectives. In cases where several objectives are involved, the problem is known as a multi-objective optimization (MOO). The objectives of any project or process are generated based on the problems or limitations associated with it. For instance, in a typical construction project, the challenges involved are budget and time constraints, safety, health, quality, etc. As such, a construction project involves multiple objectives including productivity maximization, safety and health, minimum duration and cost. The combination of these objectives should be considered for an optimal solution to the construction project. The approach of MOO is adopted over a single objective since in most real industrial processes, optimizing one aspect (parameter) has a direct influence on the other parameters and therefore could cause conflicts among the optimized and other parameters [1].

In the fused deposition modelling (FDM) process, the objective is to achieve low surface roughness, high mechanical strength, low defect density (such as cracks

F. M. Mwema and E. T. Akinlabi, *Fused Deposition Modeling*,
Manufacturing and Surface Engineering,
https://doi.org/10.1007/978-3-030-48259-6_3

and porosity), thermally stable prints, dimensionally accurate products, reduce on printing time, material cost, just to mention a few. As such, just like other manufacturing processes, fused deposition modelling is a multi-objective problem and requires the MOO approach for optimal process and product quality. There are so many MOO methods utilized across various fields, some of them include Genetic algorithms (GA), Differential evolution (DE), Pareto evolutionary algorithm (PEA), Non-dominated sorting genetic algorithm-II (NSGA-II), Particle swarm optimization (PSO), Hungarian algorithm (HA), Analytic network process (ANP), Hybrid methods, among so many other techniques.

3.2 Theory of Multi-optimization Techniques

Multi-objective optimization (MOO) deals with minimization or maximization of a vector objective $F(x)$ subject to equality $(h_l(x))$ and inequality $g_k(x))$ constraint functions. The problem for MOO is generally formulated as illustrated by Eqs. (3.1) and (3.2).

Optimize

$$f(x) = [f_1(x), f_2(x), \ldots f_k(x)]^T \tag{3.1}$$

$$f(x) \in R^k, (x) \in R^n \tag{3.2}$$

Subject to equality and inequality constraint functions as defined by Eqs. (3.3) and (3.4).

$$g_k(x) \leq 0, k = 1, 2, \ldots m \tag{3.3}$$

$$h_l(x) \leq 0, l = 1, 2, \ldots p \tag{3.4}$$

The $F(x)$ is also subject to side constraints ($x_j^{\inf}$ and $x_j^{\sup}$) in n-dimensional real space defined in Eq. (3.5).

$$x_j^{\inf} \leq x_j \leq x_j^{\sup}; j = 1, 2, \ldots n \tag{3.5}$$

where x is a vector of decision variables $[x_1, x_2, \ldots, x_n]$ and the problem is considered in two-dimensional Euclidean space (where n is the dimensional space of the decision variables and k is the dimensional space of the objective functions). The objective is to determine the set of vectors which satisfy g_k and h_l and the particular set of values of $x_1, x_2, \ldots, x_n$ which yield the optimum values of all the objective functions. These constraints define the feasible region as shown by Eq. (3.6).

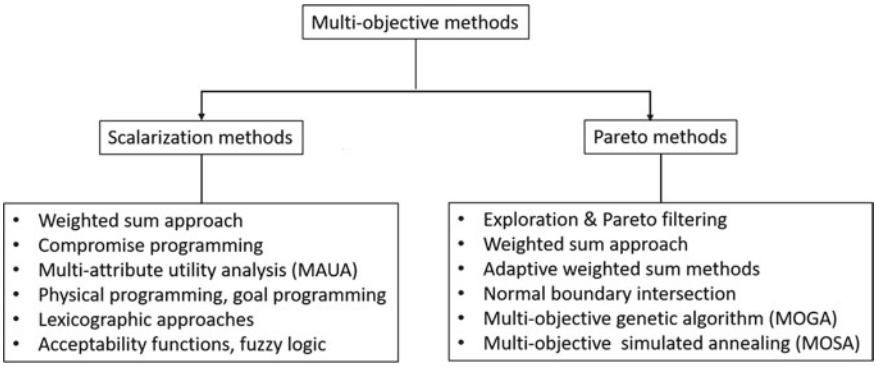

Fig. 3.1 Classification of multi-objective optimization (MOO) methods

$$\Omega = \left\{ x \in R^n / g_{(x)} \leq 0;\ h_{(x)} = 0 \right\} \tag{3.6}$$

In most cases, the components of the vector $F(x)$ (objective function) will compete with each other and therefore, such problems will have several solutions. The dilemma lies in the choice of the solution for the optimization problem. To determine an optimal solution, one must find the minimum attainable for all the objective functions separately. The Pareto method of non-dominated solutions is one of the methods to determine the optimal solution for a set of competing objective functions [2]. Pareto optimality enables us to determine the 'trade-offs' rather than single solutions for multi-objective problems [3]. Some of the classical methods of multi-objective optimization include scalarization (weighting), hierarchical, trade-off, global criterion and goal programming methods [3]. Multi-objective evolutionary algorithms (MOEAs) have been developed to advance these classical methods. According to Weck (2004), the MOO techniques can be broadly classified into scalarization and Pareto methods as summarized in Fig. 3.1 [4]. The two methods are briefly described here to provide insights into the basics of MOO process and this is illustrated in the next section with case studies of fused deposition modelling.

3.2.1 Pareto Methods

The Pareto method determines the most efficient solutions from a set of feasible solutions which arises from conflicting objective functions. Pareto improvement involves movement of one feasible solution to another that can make (i) at least one objective function to return a better value and (ii) with no other objective function becoming worse off. In this process, the elements of the solution vectors are kept independent from each other and the principle of dominance is adopted to differentiate the dominated and non-dominated solutions. Once the solutions are chosen such that changes in one objective function influence the other objective function, the solution is called

Pareto optimal solution. Generally, Pareto optimality solutions are obtained as per the following major steps: (i) Determination of the feasible solutions for maximization or minimization of objective functions, (ii) Undertaking non-dominating sorting, (iii) Determination of Pareto front and assignment of ranks to populations of solutions and finally (iv) For each rank of population, determine the crowding distance. Usually, solutions in rank 1 are non-dominated and dominate all the other sets in the solution populations. Additionally, solutions in each rank have the same fitness and solutions in rank 1 exhibit the highest fitness. In determining the 'preferred' solution from each rank, sets lying in less-crowded areas are chosen and this means that those with the largest crowding distance are chosen. Readers are referred to [5] for further description of the Pareto method.

3.2.2 Scalarization Method

In this method, the multi-objective problem is converted into a single-objective solution before the optimization process starts. The objective function is assigned various contributions (weights) to form a weighted sum of all the objectives as shown in Eqs. (3.7) and (3.8).

$$f(x) = \sum_{i=1}^{k} w_i f_i(x) r_i \tag{3.7}$$

where

$$\sum_{i=1}^{k} w_i = 1 \tag{3.8}$$

r_i are constant multipliers, $w_i \geq 0$ are weighting coefficients that show the relative significance of each choice. Usually, the challenge is attaching the weights to various objectives and determining their importance. It is important to ensure that the units of the weights are approximately the same as the numerical values of all the functions. The best results are obtained if the multiplier (r_i) is an inverse of the ideal solution (f_i^0).

3.3 Case Studies in Optimization of FDM

As mentioned, fused deposition modelling (FDM) can be approached as a multi-objective optimization problem. For example, just like any other manufacturing process, the objective of any FDM manufacturer is to minimize production time,

cost and material wastage. In this section, some case studies (from the literature) on multi-objective optimization of the FDM processes are discussed with emphasis on the MOO techniques utilized. The overall aim is to illustrate the MOO approach as a strategy for quality enhancement in FDM manufacturing.

3.3.1 Case 1: Non-dominated Sorting Genetic Algorithm-II (NSGA-II)

A study by Asadollahi-Yazdi et al. [6], titled 'Multi-Objective Optimization of Additive Manufacturing Process', is one of the classic case studies in the multi-objective optimization of fused deposition modelling (FDM). There were two objective functions formulated in the study namely, production time and material mass, two decision variables namely layer thickness and part orientation were chosen, and surface roughness and mechanical strength of the prints were considered as the constraint functions. The objective of any manufacturing process, including FDM, is to minimize the time of production and material utilization to achieve the lowest cost. These two objectives are influenced by process parameters of which the literature has shown that orientation and layer thickness are the most significant and as such were chosen as the decision variables in this research. However, the extent to minimize both time and material utilization during the FDM process is constrained by surface roughness (Ra) and mechanical strength (UTS) of the printed product. The orientation angles (θ_x, θ_y and θ_z) of the part in space in relation to *X*-, *Y*- and *Z*-axes were specified as follows: varying between -180° and 180° for *X*- and *Z*-axes while for Y-axis was chosen between 0° and 180°. With the minimum and maximum layer thicknesses defined as L_{tmin} and $L_{tmax,}$ respectively, the multi-objective optimization problem of this study was formulated according to Eqs. (3.9)–(3.15):

Minimize

$$f_1(x) = \text{Time}(x) \tag{3.9}$$

$$f_2(x) = \text{Material}(x) \tag{3.10}$$

Under the constraints:

$$g\,R_a(x) \leq R_{a\max} \cdots \text{(surface roughness constraint)} \tag{3.11}$$

$g_{\text{UTS}}(x) \geq \sigma_{\max}$ (mechanical behaviour of AM products, ultimate tensile strength (UTS)).

$$l_b \leq x \leq u_b \tag{3.12}$$

With

$$x = \left[\theta_x, \theta_y, \theta_z, L_t\right] \tag{3.13}$$

$$l_b = \left[-180°, 0°, -180°, L_{\text{tmin}}\right] \tag{3.14}$$

$$u_b = \left[180°, 180°, 180°, L_{\text{tmax}}\right] \tag{3.15}$$

The upper and lower bounds of the decision variable (x) were defined as u_b and $l_{b,}$ respectively. Based on the various parameters, an experimental study involving slicing and 3D printing of the parts at different orientations and layer thicknesses was undertaken. The manufacturing time and material usage were determined from the slicing software whereas the constraints were measured on the printed parts, i.e. surface roughness and mechanical strength. Non-dominated sorting genetic algorithm II (NSGA-II) technique was applied to determine the optimal manufacturing conditions of the sample printed product (bag hook in this case). The generated population of solutions was evaluated through the Pareto optimal non-dominated front plots for the two objective functions followed by crowding distance computations for different rankings of solutions. The approach was shown to be effective for achieving optimal manufacturing cost and quality products during the FDM process.

3.3.2 Case 2: Signal-to-Noise and Grey Correlation Degree Multi-objective Optimization

A 'multi-objective optimization of process parameters for biological 3D printing composite forming based on SNR and grey correlation degree' undertaken by Jiang et al. in 2015 [7] is another important case study. The study aimed at achieving quality objectives to enhance the quality of 3D printed scaffolds, namely, wire width and layer height errors. The study utilized signal-to-noise ratio to compute the uncertainties in the process and grey relational method for multi-objective optimization. The study was based on an orthogonal multilevel method consisting of six parameters and five levels ($L_{25}(5^6)$ orthogonal array). The parameters considered were platform velocity, extrusion speed, fibre spacing, electrospinning concentration, acceptance distance and voltage. The multi-objective optimization problem in this study was formulated as follows.

The objective of the optimization was to minimize the errors in width and layer height during the 3D printing of biological scaffolds. As such, the formulation is represented by Eqs. (3.16) and (3.17).

Minimize

$$f_1(x) = w_{\text{error}}(x_i);\ i = 1, 2, \ldots, 25 \tag{3.16}$$

$$f_2(x) = l_{\text{error}}(x_i); i = 1, 2, \ldots, 25 \tag{3.17}$$

where $f_1(x)$ and $f_2(x)$ denote the objective functions for width error (w_{error}) and layer height error (l_{error}), respectively. From the objective functions, x_i indicates the actual values of the objective functions at each experiment and i denotes the number of the test runs, which varied between 1 and 25. A set of measurements were obtained on the 25 experiments according to the design of the experiment (orthogonal array) from which the errors in width and layer height were determined. The signal-to-noise ratios for each of the objective functions at each experiment were determined using the 'smaller-the-best' criterion since the aim was to minimize the errors.

The grey relation modelling was undertaken on the SNR results for the two objective functions as illustrated in the chart in Fig. 3.2.

As shown in Fig. 3.2, the grey relation coefficient (GRC), grey relation grade (GRG) and average grey correlation degree were the outputs of the grey relation model. Based on the model and SNR methodology, the following conclusions can be deduced, which can be adopted as strategies for quality enhancement of the FDM process.

- The sequence of the influence of the specific control parameters was determined from which the material extrusion speed was identified as the most influential parameter determining the accuracy of the 3D printing of biological scaffolds. The sequence of the other parameters was as follows: platform velocity, accepting distance, electrospinning concentration, voltage and fibre spacing. The voltage and fibre spacing were the least significant parameters influencing the accuracy of the scaffolds. A survey of the literature shows very few studies investigating the influence of these two parameters on the quality of FDM products. This could be attributed to the fact that the parameters have minimal influence on the process and hence the quality of the products. The speeds of both the extruder and the build plate are identified as very important factors during FDM. These parameters affect melting and fusion of the filament during the process. If proper speeds are not chosen, the staircasing effect and formation of cusps may occur resulting in improper fusion and hence inaccurate height and width of the layers. In fact, the

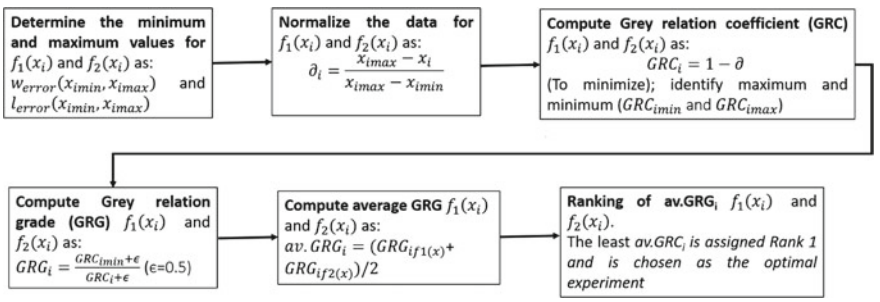

Fig. 3.2 Summary of the grey relation model optimization adopted by Jiang et al. [7]

layer thickness has a direct relationship with the staircase; that is, the larger the layer thickness, the larger the staircase effect and hence, the poor the surface quality of the prints [8].

- According to the grey relation model, the optimum combination of the parameters was extrusion speed of 16 mm/s, plate speed of 16 mm/s, electrospinning concentration of 8.7%, voltage of 19 kV, fibre spacing and accepting distance of 1.4 mm and 100 mm, respectively. The model optimization was confirmed through an experiment undertaken under the optimum conditions and high-quality biological scaffolds were produced.

3.3.3 Case 3: Particle Swarm Optimization Method for Fused Deposition Modelling Process

A particle swarm optimization (PSO) method was utilized by Dey, Hoffman and Yodo in 2019 in their paper titled, 'optimizing multiple process parameters in FDM with PSO' [9]. In their investigation, four decision variables namely build orientation, infill density, extrusion temperature and layer thickness were tested. Additionally, two objective functions namely compressive strength and printing time were used. As mentioned earlier, the objective FDM process is to reduce the manufacturing time and enhance the strength of the printed products. These are two major aspects limiting industrial and mass production adoption of additive manufacturing technologies. Each of the process parameters had three levels; a face-centred central composite design (FCCCD) design of the experiment was applied to the array (3^4). This approach belongs to a group of DOE methods called response surface model (RSM). As such, the minimum and optimal number of experiments used from the FCCCD design was 30 experiments.

Particle swarm optimization (PSO) is a meta-heuristic optimization procedure that is inspired by natural behaviour of birds, fish and plants in their natural setting especially in search of water, food and sunlight and it was developed by Kennedy and Eberhart in 1995 [10]. The algorithm takes each of the solution candidates in the solution space as a particle in a swarm and the optimization involves the iterative improvement of each candidate with respect to a given measure of quality. Within the solution space, each particle has velocity and position which the algorithm uses to obtain the optimal points. The equations describing position (X) and velocity (V) are represented by Eqs. (3.18) and (3.19), respectively.

$$V_i(t+1) = \omega V_i(t) + c_i r_i(t)(P_i(t) - X_i(t)) + c_2 r_2(t)(g(t) - X_i(t)) \tag{3.18}$$

$$X_i(t+1) = X_i(t) + V_i(t+1) \tag{3.19}$$

where ω is the inertia coefficient, c_i and c_2 represent the cognitive and social acceleration coefficients (learning factors) respectively, r_1 and r_2 are random numbers

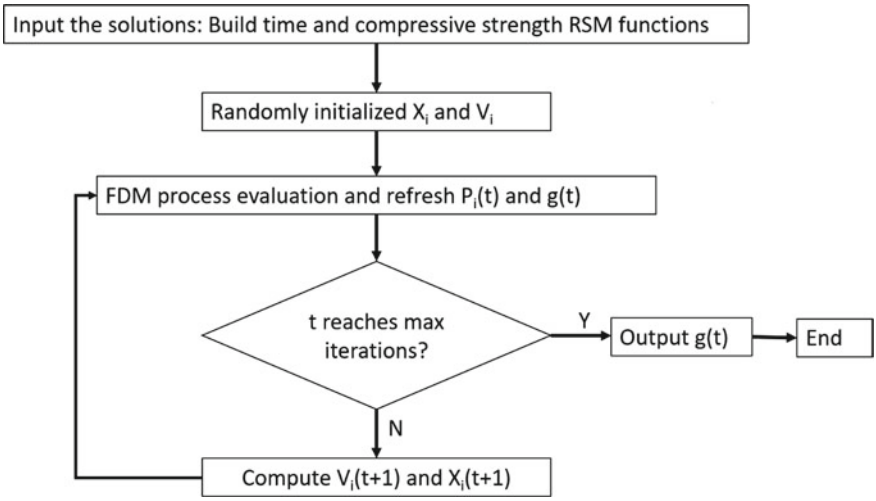

Fig. 3.3 Flow chart of the PSO methodology utilized by [9]

varying between 0 and 1. Also, $P_i(t)$ and $g(t)$ represent the best location (best experience) of each particle and the best common location (global best) for all the particles, respectively. In fact, the function $g(t)$ represents the minimum global (optimal) point of all the particles in the swarm.

In this study, the following step-by-step procedure (Fig. 3.3) for PSO multi-objective optimization was implemented according to study [11].

As shown in Fig. 3.3, the response surface quadratic modelling was applied to determine the relationship among the FDM parameters and the compressive strength and build time. It was observed that the extrusion temperature was insignificant for both compressive strength and printing time. As such, the extrusion temperature was eliminated among the decision variables of the multi-objective problem. The quadratic equations (relating the decision variables to the build time and compressive strengths) were developed, which were then used as the objective functions of the particle swarm optimization. In the optimization problem, the layer thickness (mm), orientation (°) and density (%) were the decision variables whereas the parameter levels (low, average and high) were taken as the constraints. The algorithm was implemented based on the pseudocodes reported in studies [12, 13]. The result of the multi-objective particle swarm optimization (MOPSO) was a Pareto frontier to represent the trade-off between the conflicting objectives. Two main conclusions can be deduced from this study for enhanced strength and optimal time of printing of PLA samples:

- For the set of non-dominating solutions obtained, the build orientation of 0° was the best for both objectives. At this orientation, the fibres of the PLA are layered parallel to the direction of the compressive load and therefore they provide the best resistance to loading as compared to 45° and 90°.

- At 0° printing orientation, the printer achieves the required thickness at a lower number of layers. This is because the build plate is only required to move in a downward direction when printing the subsequent layers. In other orientations, the plate may be required to incline or turn besides the downward movement, which requires a longer time for the printer to form the subsequent layers.

3.3.4 *Case 4: Full Factorial and Grey Relational Degree Optimization of FDM Printed PLA*

In this section, we present our multi-objective optimization of the study presented in Chap. 2 of this book. The experiment for the PLA printing was undertaken using a full factorial mixed-level design. The layer thickness (three levels) and build orientation (six levels) are the decision variables whereas the levels are the constraints. The objective of the process is to minimize the roughness (Ra) and printing time (t) and maximize the surface hardness (HBR). Therefore, the multi-objective optimization problem in this case is formulated according to Eqs. (3.20) and (3.21).

Objective functions: Minimize

$$f_1(x) = Ra_i(x) \tag{3.20}$$

$$f_2(x) = t_i(x) \tag{3.21}$$

Maximize

$$f_3(x) = HBR_i(x); \text{ for all the objective functions, } i = 1, 2, \ldots .18$$

The functions are subject to the following constraints of different levels of each function.

$$\text{For layer thickness, } 0.1 \leq x \leq 0.3$$

$$\text{For build orientation , } 0^\circ \leq x \leq 90^\circ$$

As detailed in Chap. 2, 18 experiments were undertaken at given constraints. However, our printer did not print at one of the conditions (45° build orientation and 0.3-mm layer resolution) and therefore there were only 17 investigations undertaken. The time of printing was determined directly from the slicing software whereas the roughness and hardness tests were undertaken on respective laboratory facilities. The obtained values of the decision variables for each function index (i) are shown in Table 3.1. A grey relational modelling was then applied to this data following the

Table 3.1 The experimental order, decision variables and objective functions

Chapter 2 exp. number	Resolution	Orientation	Ra	HBR	t (min)
1	0.1	30	3.61	124.8	24
2	0.2	15	6.88	126.9	13
3	0.1	60	2.89	126.1	24
4	0.1	45	4.04	128.3	24
5	0.1	15	5.07	127.5	24
6	0.2	30	8.8	126.4	14
7	0.2	60	8.77	127.5	13
8	0.2	45	4.35	129.4	10
10	0.1	90	1.33	127	25
11	0.2	90	2.89	124.3	15
12	0.3	60	8.44	128.9	7
13	0.3	0	4.78	127	15
14	0.2	0	2.48	130.7	18
15	0.1	0	1.51	128.6	28
16	0.3	15	6.76	130.6	10
17	0.3	30	9.08	125.5	7
18	0.3	90	8.84	124.7	11
Minimum (X_{min})			1.33	124.3	7
Maximum (X_{max})			9.08	130.7	28

general methodology in Fig. 3.2. In Table 3.1, the minimum and maximum values for each objective function were identified and are stated in the last rows of the table.

Using the minimization equation in Fig. 3.2, the normalization was undertaken for Ra and t functions whereas the normalization for maximization of HBR function was undertaken using Eq. (3.22).

$$\text{Normalization for maximization of HBR} = \frac{X_i - X_{\min}}{X_{\max} - X_{\min}} \tag{3.22}$$

Next, the grey relation coefficient (GRC) was determined for the three functions as earlier described in Fig. 3.2. However, it should be noted that for the maximization process, the values of the normalized function (HBR) represent the GRC and therefore, no transformation was applied in the data. The results of these operations are shown in Table 3.2. It can be noted that the column of HBR data is the same for both sets of data (normalized and GRC data) since it is a maximization objective.

Next, the data in Table 3.2 was transformed into a grey relational grade (GRG) and degree (rank) following the equations in Fig. 3.2. The value of $\in = 0.5$ was used in this experiment and its choice was based on the existing literature and the results of the operations are shown in Table 3.3. As shown, the grey relation model transformed

Table 3.2 Normalized data for objective functions and computation of grey relational coefficient

Normalized data				Grey relational coefficient (GRC)		
Exp. number	Ra	HBR	t (min)	Ra	HBR	t (min)
1	0.7058	0.0781	0.1905	0.2942	0.0781	0.8095
2	0.2839	0.4063	0.7143	0.7161	0.4063	0.2857
3	0.7987	0.2813	0.1905	0.2013	0.2813	0.8095
4	0.6503	0.6250	0.1905	0.3497	0.6250	0.8095
5	0.5174	0.5000	0.1905	0.4826	0.5000	0.8095
6	0.0361	0.3281	0.6667	0.9639	0.3281	0.3333
7	0.0400	0.5000	0.7143	0.9600	0.5000	0.2857
8	0.6103	0.7969	0.8571	0.3897	0.7969	0.1429
10	1.0000	0.4219	0.1429	0.0000	0.4219	0.8571
11	0.7987	0.0000	0.6190	0.2013	0.0000	0.3810
12	0.0826	0.7188	1.0000	0.9174	0.7188	0.0000
13	0.5548	0.4219	0.6190	0.4452	0.4219	0.3810
14	0.8516	1.0000	0.4762	0.1484	1.0000	0.5238
15	0.9768	0.6719	0.0000	0.0232	0.6719	1.0000
16	0.2994	0.9844	0.8571	0.7006	0.9844	0.1429
17	0.0000	0.1875	1.0000	1.0000	0.1875	0.0000
18	0.0310	0.0625	0.8095	0.9690	0.0625	0.1905
Minimum				0	0	0
Maximum				1	1	1

the three objectives into a single-objective optimization problem (average GRG). Then, the ranking (degree) shows the sequence of the significance of each index (i) in the optimization. The highest degree (rank 1) shows the most optimal setpoint of the experiment and the best trade-off.

From Table 3.3, it can be seen that the most optimal set of the solution was obtained at index ($i = 11$) or experiment no. 11 in which the values of roughness (Ra), hardness (HBR) and time of manufacturing (t) were 2.89 μm, 124.3, and 15 min, respectively (see Table 3.1). The results in Table 3.3 represent the Pareto optimality and non-dominating solutions for a multi-objective optimization problem. The result represented by rank 1 is, therefore, the Pareto optimal (non-dominated front), followed by rank 2 and so forth.

To demonstrate the relationship between the results in Table 3.3 and Pareto optimal and non-dominating frontier concepts, a three-dimensional scatter plotting of the values of roughness, hardness and time from Table 3.1 was undertaken. In this case, it was assumed that the actual laboratory values of the three objective functions represent the solution space for the multi-objective problem. Figure 3.4 shows the 3D scatter plots of the three responses. As shown in Fig. 3.4 and Table 3.3, the non-dominated frontier provides the best trade-offs among the objectives of the

Table 3.3 Computation of grey relational grade (GRG), average GRG and degree (rank)

Exp. number	Resolution	Orientation	Grey relational grade (GRG)			Average GRG	Rank
			Ra	HBR	t (min)		
1	0.1	30	0.6296	0.8649	0.3818	0.6254	5
2	0.2	15	0.4111	0.5517	0.6364	0.5331	11
3	0.1	60	0.7130	0.6400	0.3818	0.5783	7
4	0.1	45	0.5885	0.4444	0.3818	0.4716	16
5	0.1	15	0.5089	0.5000	0.3818	0.4636	17
6	0.2	30	0.3416	0.6038	0.6000	0.5151	13
7	0.2	60	0.3425	0.5000	0.6364	0.4929	15
8	0.2	45	0.5620	0.3855	0.7778	0.5751	8
10	0.1	90	1.0000	0.5424	0.3684	0.6369	4
11	0.2	90	0.7130	1.0000	0.5676	0.7602	1
12	0.3	60	0.3528	0.4103	1.0000	0.5877	6
13	0.3	0	0.5290	0.5424	0.5676	0.5463	10
14	0.2	0	0.7711	0.3333	0.4884	0.5309	12
15	0.1	0	0.9556	0.4267	0.3333	0.5719	9
16	0.3	15	0.4164	0.3368	0.7778	0.5104	14
17	0.3	30	0.3333	0.7273	1.0000	0.6869	2
18	0.3	90	0.3404	0.8889	0.7241	0.6511	3

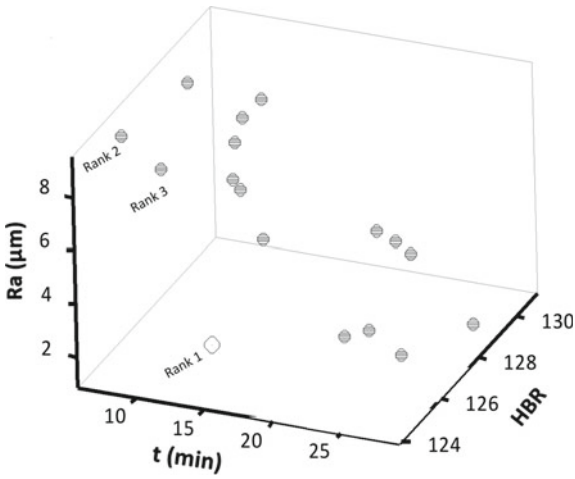

Fig. 3.4 Graphical representation of the solution candidates for the multi-objective optimization problem. The Pareto optimality (non-dominated fronts) are also shown as ranks 1, 2 and 3

optimization process. For example, comparing ranks 1, 2 and 3, it can be seen that experiment 11 dominates rank 2 (experiment 17) in terms of low roughness and high hardness except for the time of production. It can also be seen that rank 1 (experiment 11) dominates rank 3 (experiment 18) in all the objectives, i.e. using experiment 11 conditions produces FDM components at low roughness, high hardness and at a higher rate of production as compared to experiment 18. Therefore, according to the grey relation and Pareto non-dominated front models, 3D printing of PLA at a build orientation of 90° and layer height (resolution) of 0.2 mm provides the highest fitness and best conditions for low roughness, high production rate (time) and better mechanical strength (hardness).

In a related approach, grey relational models can be used in conjunction with the Taguchi optimization method to determine the influence and significance of the two decision variables used during the fused deposition modelling. The results of the GRG (reported in Table 3.3) were taken as the responses to the Taguchi optimization model and the following results were obtained (Fig. 3.5 and Table 3.4). The optimization was based on the 'larger-the-best'. As shown, the highest S/N ratios were observed at 90° and 0.3-mm build orientation and layer height (resolution), respectively. These parameters coincide with experiment 18, which was ranked third as per the grey relation modelling. The results of the ANOVA (at 95% confidence level) for the GRG show that the resolution has an insignificant influence on the GRG and hence to the roughness, time and hardness as compared to the build orientation. The P-values for orientation were around 0.03 whereas that of the resolution was 0.65. The plots of means of GRG for the two parameters are also shown in Fig. 3.6 and it further affirms the Taguchi model in this study.

The most important aspect of the Taguchi is that it undertakes a single-objective optimization and it is able to rank the significance of each processing parameter's

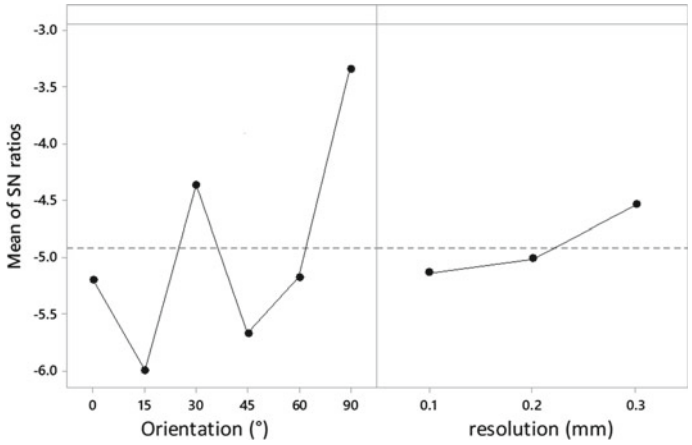

Fig. 3.5 Main effects plots for S/N ratios of the grey relation grade (GRG) for the 3D printing of PLA samples at different orientation angles and layer resolution

Table 3.4 S/N response table for GRG. The bold values indicate the maximum S/N ratios of the Taguchi optimization

Level	Orientation	Resolution
1	−5.201	−5.136
2	−5.995	−5.009
3	−4.367	−4.540
4	−5.667	
5	−5.173	
6	−3.342	
Delta	2.653	0.595
Rank	1	2

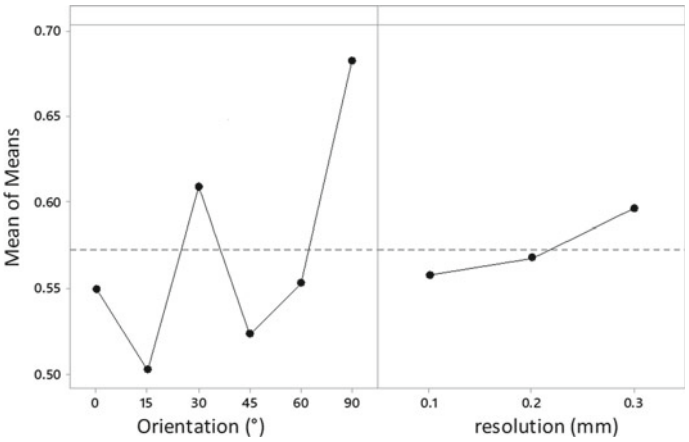

Fig. 3.6 The main effect plots of means of GRG for the 3D printed PLA samples at different levels of orientation and layer resolution

level to the quality of the 3D printing. Here, the most influential level for orientation was 90° followed by 30°, 0° and 60°, while the least significant levels were 45° and 15°. For the layer thickness, the most influential level was 0.3 while the least important level was 0.1 mm. Although the products printed at higher layer resolution exhibited very high roughness, they were shown to have better hardness and lower time of printing. At a larger layer thickness, higher rate of filament material is extruded and hence the required print thickness is achieved quickly as compared to when a smaller layer resolution is utilized. Furthermore, during the manufacturing of rectangular samples, such as those illustrated in this work, either 0° or 90° angles are observed as the best printing orientations. However, their choice will depend on layer resolution and the best trade-off for the decision makers. A trade-off has to be made between productivity rate and surface quality/strength of the samples (Table 3.5).

Table 3.5 Results of ANOVA for grey relation grade (GRG)

Source	DF	Adj SS	Adj MS	*F*-value	*P*-value
Regression	3	0.0.35	0.012	2.27	0.129
Orientation	1	0.031	0.030	5.96	0.030
Resolution	2	0.005	0.002	0.45	0.647
Error	13	0.067	0.005		
Total	16	0.101			

3.4 Summary

In this chapter, case studies have been used to illustrate the multi-objective optimization (MOO) approach as a strategy for quality achievement of the fused deposition modelling process. Time of printing, surface and mechanical integrity are the main objectives for the MOO process. Some of the MOO techniques which have been used in the FDM process are NSGA-II, Taguchi-Grey relational degree, Particle swarm optimization (PSO) and Pareto optimization methods. Usually, the decision variables in the FDM process are the 3D printing parameters such as temperature, speed, infill density, build orientations, layer thickness, among others.

References

1. N. Gunantara, A review of multi-objective optimization: Methods and its applications. Cogent Eng. **5**(1), 1–16 (2018)
2. L.S. de Oliveira, S.F.P. Saramago, Multiobjective optimization techniques applied to engineering problems. J. Braz. Soc. Mech. Sci. Eng. **32**(1), 94–105 (2010)
3. C.A.C. Coello, Multi-objective optimization. In: *Handbook of Heuristics* (Springer International Publishing, Cham, 2018), pp. 1–28
4. O.L. de Weck, Multiobjective optimization : History and promise. In: *Proc. 3rd China-Japan-Korea Joint Symp. Optimization Structural Mech. Syst. Invited Keynote Paper GL2-2* (2004), p. 14
5. C. Saule, R. Giegerich, Pareto optimization in algebraic dynamic programming. Algor. Mol. Biol. **10**(1), 1–20 (2015)
6. E. Asadollahi-Yazdi, J. Gardan, P. Lafon, Multi-objective optimization of additive manufacturing process. IFAC- Pap. Online **51**(11), 152–157 (2018)
7. Z. Jiang, Y. Liu, H. Chen, Multi-objective optimization of process parameters for biological 3D printing composite forming based on SNR and grey correlation degree. 3–8 (2015)
8. M.A. Matos, A.M.A.C. Rocha, A.I. Pereira, Improving additive manufacturing performance by build orientation optimization. Int. J. Adv. Manuf. Technol. (2020)
9. A. Dey, D. Hoffman, N. Yodo, Optimizing multiple process parameters in fused deposition modeling with particle swarm optimization. Int. J. Interact. Des. Manuf. No. 0123456789 (2019)
10. R. Ceylan, H. Koyuncu, ScPSO-based multithresholding modalities for suspicious region detection on mammograms. In *Soft Computing Based Medical Image Analysis* (Elsevier, 2018), pp. 109–135

11. S. Lalwani, S. Singhal, R. Kumar, N. Gupta, a comprehensive survey: applications of multi-objective particle swarm optimization (Mopso) algorithm. Trans. Comb. ISSN **2**(1), 2251–8657 (2013)
12. C.A. Coello Coello, G.T. Pulido,M.S. Lechuga, Handling multiple objectives with particle swarm optimization. IEEE Trans. Evol. Comput. **8**(3), 256–279 (2004)
13. N. Kim, I. Bhalerao, D. Han, C. Yang, and H. Lee, Improving surface roughness of additively manufactured parts using a photopolymerization model and multi-objective particle swarm optimization. Appl. Sci. **9**(1) (2019)